CHAPTER 2

Cytochrome c Peroxidase–Cytochrome c Complexes

THOMAS L. POULOS

Departments of Molecular Biology & Biochemistry, Pharmaceutical Sciences, and Chemistry, University of California Irvine, Irvine, California 92697-3900, USA
Email: poulos@uci.edu

2.1 Initial Studies

An excellent comprehensive review on the yeast cytochrome c peroxidase–cytochrome c complex was published in 2011[1] so in this chapter, the discussion on earlier work will be limited to that most relevant to more current insights. Yeast cytochrome c peroxidase (CCP) was first described in 1940[2] but it was not until the mid-1960s when Yonetani and colleagues streamlined the purification process that real advances were made. An early review published in 1976 summarizes much of these initial efforts.[3] Compared to other peroxidases, especially horseradish peroxidase (HRP), CCP was unusual since Compound I does not form the characteristic green porphyrin π cation radical typical of HRP and catalase.[4] Instead, the reaction between one equivalent of H_2O_2 and CCP gives a red intermediate that exhibits an intense $g \approx 2.0$ EPR signal.[5] Since this was so different to HRP Compound I, this intermediate was called Complex or Compound ES but in this chapter we will refer to this red EPR active intermediate as Compound I. Allowing Compound I to spontaneously decay resulted in the destruction of Tyr and Trp residues so it was correctly concluded that the EPR species in Compound I is very likely an aromatic amino acid radical.[6] Later on, elegant isotope

RSC Metallobiology Series No. 4
Heme Peroxidases
Edited by Emma Raven and Brian Dunford

Published by the Royal Society of Chemistry, www.rsc.org

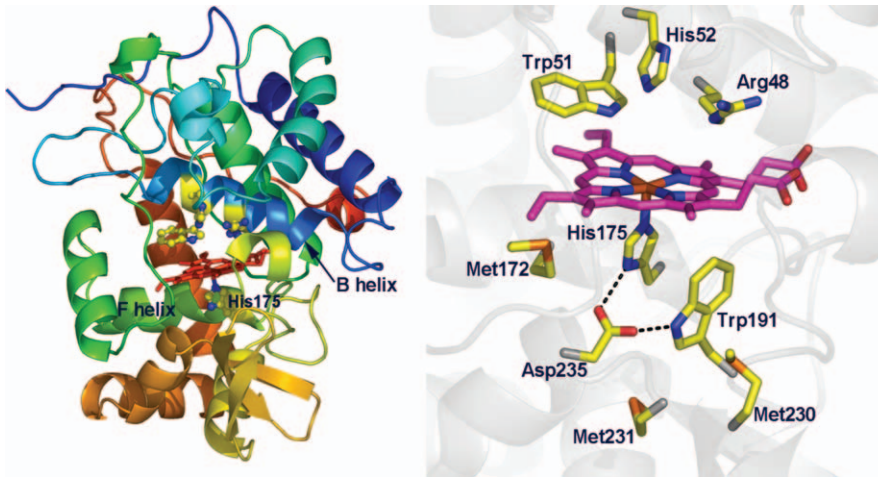

Figure 2.1 Crystal structure of yeast cytochrome c peroxidase. The overall fold is highly conserved among plant, fungal, and mitochondrial peroxidases. The heme binds in a cleft between the N- and C-terminal domains sandwiched between the F and G helices. The heme is coordinated to a His ligand which, in turn, H-bonds with the conserved Asp235. In the distal pocket, His52 and Arg48 play important roles in Compound I formation.

substitution and spectroscopic studies showed that the radical resides on Trp191[7] (Figure 2.1).

In addition to the unusual free radical properties of Compound I, CCP also differed from other peroxidases in that the reducing substrate is another heme protein, cytc, rather than small aromatic compounds more typical of plant peroxidases. Since CCP was relatively easy to prepare and cytc was commercially available, the CCP–cytc system became a paradigm for inter-protein electron transfer. In addition, CCP was the first heme enzyme crystal structure to be solved[8] while the cytc structure already had been determined[9] so there was a structural underpinning to guide the interpretation of bio-chemical and modeling experiments. Both kinetic and direct biophysical binding studies clearly showed that CCP and cytc form a complex (reviewed in ref. 1). CCP, however, does not exhibit simple Michaelis–Menten kinetics and Eadie–Hofstee plots showed a clear break (Figure 2.2) suggesting two binding sites. Indeed, direct binding studies showed that there is one weak and one strong binding site.[10,11] We will shortly address the question on whether there are one or two competent electron transfer sites.

2.2 CCP–cytc Structure

There are very few crystal structures (Table 2.1) of redox complexes because Nature has designed redox protein complexes to be transient and weak, a requirement for maintaining high turnover rates but an obstacle to

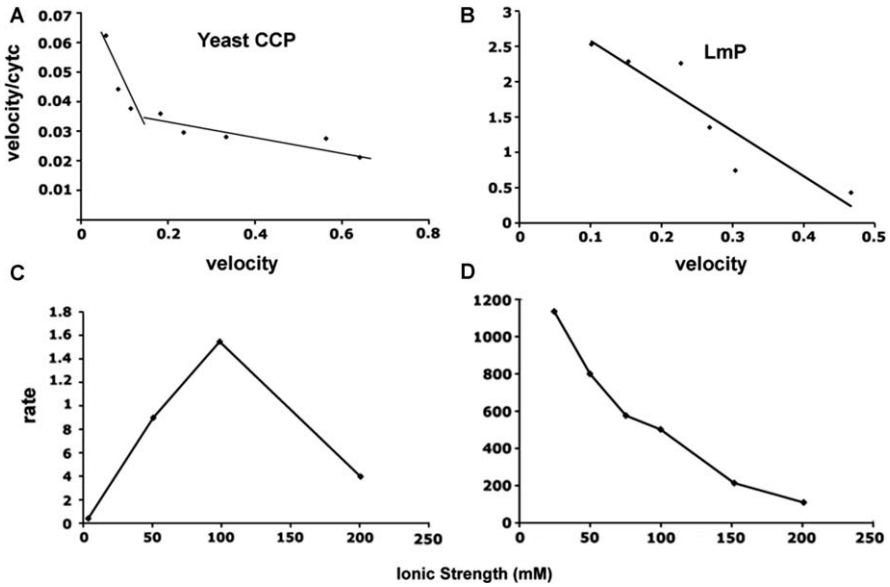

Figure 2.2 Kinetic plots of CCP and LmP adapted from the literature.[38,44] A and B are Eadie–Hofstee plots. The break in the plot for CCP indicates two cytc binding sites. C and D show the ionic strength dependence on activity. The increase in rate with ionic strength for CCP is consistent with nonpolar interactions playing an important role in complex formation.

obtaining crystals. The problem is illustrated in Figure 2.3. To ensure rapid binding, the two surfaces are electrostatically complementary which enables the association rate, k_1, to be fast on the order of 10^8 M^{-1} s^{-1}. Since rapid turnover must be maintained, the complex cannot be too tight and the K_D is usually in the 10^{-6}–10^{-5} M range, which means the off-rate, k_2, is about 10^3 s^{-1}. Since electron transfer rates fall off exponentially with distance, it is necessary for the proteins to align properly, which is illustrated by the darker ''active'' surface areas. If we are generous and say that 10% of each surface is active, then 1% of the random encounters will generate an active complex. With an off-rate of 10^3 s^{-1}, the fastest turnover possible if the active areas associate *via* a random collision process is 10 s^{-1}. However, many ET rates are in the 10^2–10^3 s^{-1} range so clearly these reactions do not proceed by random collisions. To explain this discrepancy it is generally thought that the proteins form an initial encounter complex and then sample each other's surfaces (rate constant k_2) until the productive complex is reached. To maintain high turnover, the stability of the active complex cannot be too different from the initial ''random'' encounter complex. The transient nature of these complexes and the rather shallow energy minimum for the active complex are why there are so few crystal structures.

The first attempt at solving the crystal structure of the CCP–cytc complex was reported in 1987.[12] While SDS electrophoresis showed that both proteins were in the crystal, only CCP was visible although there was sufficient

Table 2.1 A list of strucutres of protein–protein redox complexes.

Complex	PDB Code	Comments
Yeast CCP–Cytc	2PCC, 2PCB, 2GB8, 1S6V	Various versions of the yeast CCP–cytc complex including crosslinked complex
Yeast cytc–cytbc1	1KYO	Fab used to stabilize complex
P. putida putidaredoxin and putidaredoxin reductase	3LB8	Crosslinked
Pseudomonas ferredoxin and ferredoxin reductase (BphA3-BphA4)	2YVJ	
Z. mays ferredoxin and ferredoxin–NADP + reductase	1GAQ	
A. xylosoxidans copper-containing nitrite reductase and Cytc c551	1ZON	
P. denitrificans methylamine utilization protein MauG and methylamine dehydrogenase (MADH)	3L4M	
P. pantotrophus sulfur dehydrogenase (SoxC) and mono-heme cytochrome ($SoxD_1$)	2XTS	
A. faecalis aromatic amine dehydrogenase and azurin	2IAA	
H. sapiens medium chain acyl-CoA dehydrogenase (MCAD) and electron transfer flavoprotein (ETF)	1T9G	
P450cam–putidaredoxin complex	4JX1, 2M56, 3W9C	Crosslinked and non-crosslinked crystal structures and NMR structure
Leishmania major peroxidase–cytc	4GED	
Adrenodoxin–adrenodoxin reductase	1E6E	Crosslinked
P45011A1–adrenodixin complex	3N9Z, 3NA0, 3NA1	

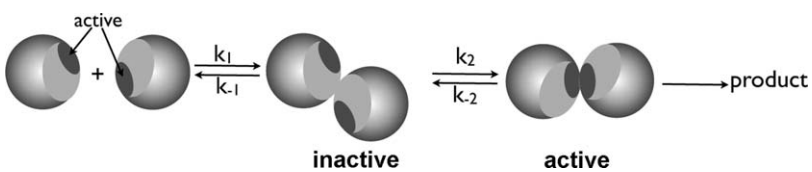

Figure 2.3 Schematic diagram illustrating one possible process for electron transfer complex formation. The large shaded area represents complementary surfaces that enable rapid formation of the initial complex. The darker shaded area represents the active surface. k_2 is the rate at which the two proteins sample each other's surface before settling down to the most stable active complex.

room in the crystal lattice for cytc. This was taken as evidence that cytc was orientationally disordered and was not rigidly fixed in a single binding mode. A few years later, Pelletier and Kraut[13] succeeded in solving the CCP–horse heart cytc structure using the same crystal form reported previously but this time, cytc was visible, presumably by allowing the crystals to partially dehydrate. Dehydration is generally thought to promote tighter protein–protein interactions, which results in increased ordering and better diffraction. The CCP–yeast cytc structure was also solved.

The structure of the yeast CCP–cytc complex is shown in Figure 2.4A and C. The structure of the crosslinked version of the CCP–cytc complex has also been solved at higher resolution,[14] which enabled visualization of solvent at the interface but otherwise, the structures are the same. To form the crosslink, Val197 in CCP and Ala81 in cytc were converted to Cys residues. The resulting S–S bond was so stable that it could only be broken after denaturation. Perhaps the biggest surprise is the lack of any ionic interactions between the two redox partners. It had been well established that the ring of positive charges surrounding the exposed heme edge of cytc is important for binding, clearly implicating electrostatic interactions as a critical feature in complex formation.[15] However, the ionic strength dependence on the reaction shows an increase in rate with increasing ionic strength (Figure 2.2C) and then a decrease. The initial increase in rate is consistent with nonpolar interactions playing an important role in complex formation and indeed, the structure does reveal some close nonbonded contacts. Moreover, a thermodynamic analysis of the CCP–cytc interactions shows that the heat capacity decreases while ΔS increases,[16] both consistent with nonbonded interactions playing a key role.

As noted earlier, in order to maintain rapid turnover, the electron transfer complex needs to be short lived and relatively weak. In addition, the crystal structure represents one of possibly many initial encounter complexes. Elegant paramagnetic enhancement NMR experiments coupled with Monte Carlo calculations have provided a dynamic picture of the CCP–cytc interaction.[17] This method requires covalently labeling engineered Cys residues in CCP with paramagnetic compounds. The relaxation of cytc amide nuclei are then measured, which provides distance information. The dynamic picture emerging from these studies is that cytc samples about 15% of the CCP surface centered roughly on the site observed in the crystal structure and the difference in stabilization between the productive and nonproductive complexes is only 0.5 kcal mol^{-1}. The majority of the complexes are not capable of fast electron transfer since the cytc heme is too far from the site of reduction in CCP, the Trp191 cation radical. This supports the ''bind and crawl'' mechanism wherein a very fast association rate is assured but at the expense of many nonproductive orientations of cytc on CCP. The cytc then samples the surface of CCP in a two dimensional ''crawl'' until the most stable complex capable of fast electron transfer is reached but since this productive complex is only marginally more stable than others, rapid disassociation and fast turnover is assured.

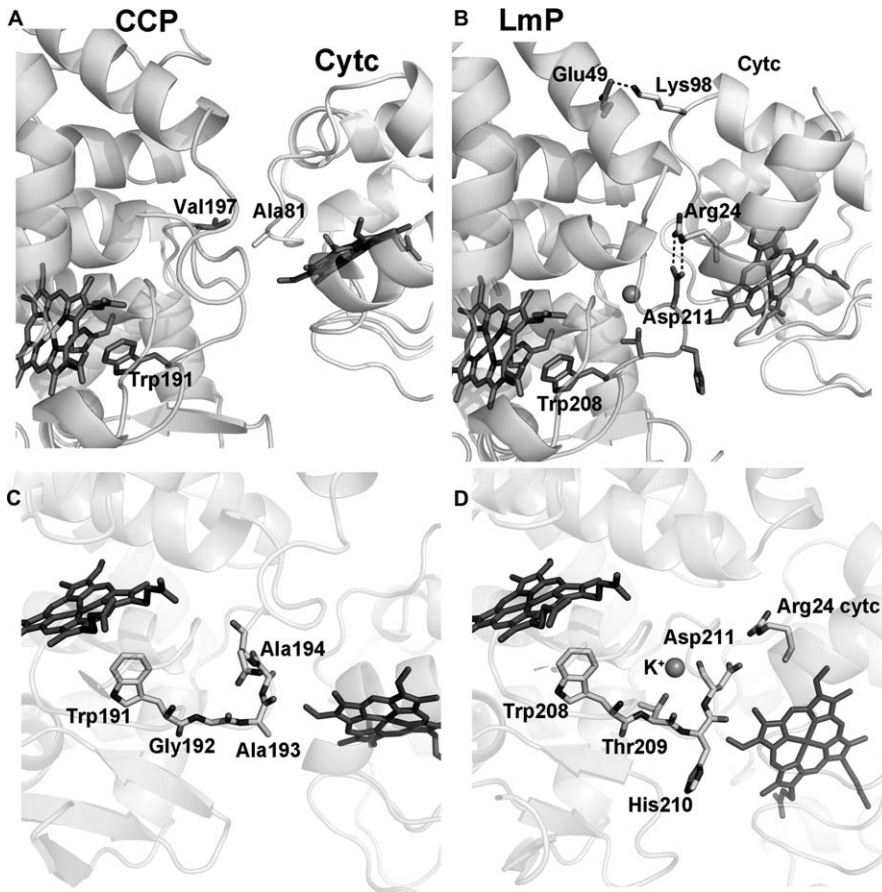

Figure 2.4 Crystal structures of the CCP–cytc (A and C) and LmP–cytc (B and D) complexes. Cytc binds to the same surface in both CCP and LmP but relative to the CCP–cytc complex, cytc rotates in the LmP–cytc complex. Nonpolar interactions play an important role in the CCP–cytc interaction while ionic interactions are more dominant in the LmP–cytc interaction, which is consistent with the kinetic data. The most important ionic interaction in the LmP–cytc complex is between Arg24 in cytc and Asp211 in LmP.

2.3 One Site or Two?

The CCP–cytc structure was generally accepted as physiologically relevant and supported by biochemical data, but the question of whether or not there are two electron transfer competent binding sites remained. A two-site scenario is attractive since there are two sites that require reduction, Fe(IV)=O and $Trp^{\bullet+}$. An important computational study provided the first structural insights into possible binding sites prior to the availability of the CCP–cytc structure. Northrup *et al* used Brownian dynamics (BD) to study the CCP–cytc complex.[18] BD differs from molecular dynamics (MD) in that

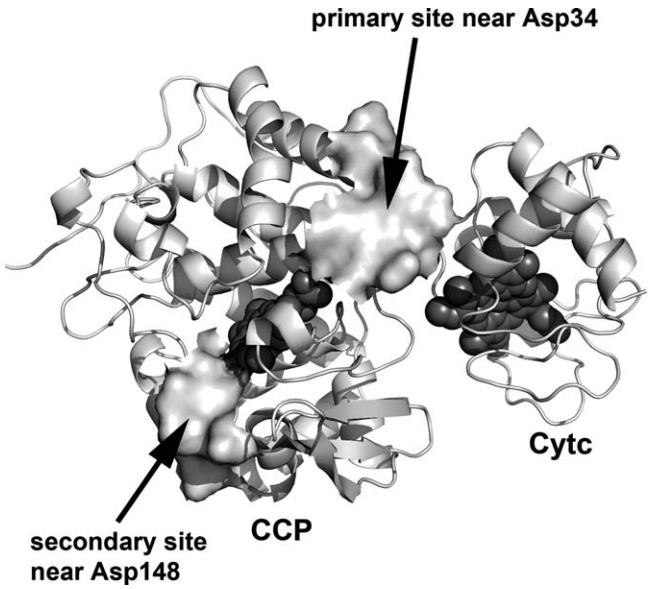

Figure 2.5 The CCP–cytc crystal structure showing the surfaces on CCP that were found to interact with cytc using Brownian dynamics.[18]

the proteins are treated as rigid particles while molecular dynamics allows all atoms to move. BD thus is a computationally inexpensive approach for following the dynamic behavior of proteins in solution on time scales that cannot be achieved by traditional MD. This allows one to follow the binding of two proteins in solution and even calculate association rate constants. This initial *tour de force* BD effort predicted two binding regions (Figure 2.5). The favored site is centered on a cluster of negative charges on Asp34 in CCP (Figure 2.5). A secondary site was found near Asp148.

To test if this second site might be functionally important, CCP and cytc were engineered to have surface Cys residues[19,20] and intermolecular S–S disulfide bond formation thus will create a CCP–cytc covalent crosslink. Crosslinking Lys149Cys in CCP to Lys79Cys in yeast cytc will block the secondary site found by the BD simulations. The rate of intramolecular electron transfer from the covalently attached cytc to the CCP Compound I Trp191 radical was found to be extremely slow (0.5–1.0 s^{-1}) while the steady state activity ranged from 50–100% of wild type activity depending on the exogenous cytc concentration and buffer conditions. This experiment showed that the Asp148 region identified by the BD simulations is not important for activity. In sharp contrast, a second crosslinking site designed to block the cytc binding region found in the crystal structure exhibited only 2–3% wild type activity while electron transfer from the covalently attached cytc to the Trp191 radical was at least 500–800 s^{-1} and probably faster since this was near the limits detectable by stopped flow spectroscopy. This type of approach was later fine-tuned by carefully designing an intermolecular

crosslink (S–S bond) near the center of the CCP–cytc interface, which was formed in such high yield and purity that the crystal structure was solved and shown to be the same as the noncovalent complex.[14] This complex also exhibited just a few percent wild type activity while electron transfer from the covalently attached cytc to the Trp191 radical was fast. It was later shown that the low activity of the crosslinked complex was due to a minor contamination of noncrosslinked CCP and that the highly purified crosslinked complex has no activity.[21] Taken together, these studies showed that CCP has only one competent electron transfer site, which is the one identified in the crystal structure. This, however, does not mean there is only one site for cytc binding. A thorough analysis of steady state data supports a two-site model but with only one being competent in electron transfer.[22] This will be discussed further in the next section.

2.4 Electron Transfer

The actual electron transfer event is not rate limiting so extracting out the rate of electron transfer from the cytc heme to Trp191$^{\bullet+}$ is not possible with steady state or even stopped flow kinetics. Millett and coworkers, in a series of elegant papers, used laser flash coupled with stopped flow methods to work out not only the rate of electron transfer but which species is reduced first: the Trp191 radical or Fe(IV)=O. Both laser induced photo-reduction[23,24] and stopped flow[25,26] showed that the Trp191 radical is reduced first. To actually capture the cytc-to-Trp$^{\bullet+}$ electron transfer reaction, it was necessary to covalently attach a photo-active ruthenium compound to the surface of cytc (Figure 2.6). A laser pulse generates an excited state Ru(II)* that rapidly transfers an electron to cytc. A sacrificial donor must be included to reduce Ru(III) back to Ru(II), otherwise the photo-generated Fe(II) in cytc will send an electron back to Ru(III). The actual rate of electron transfer from cytc to the Trp191 radical, k_{et} in Figure 2.6, is about 2×10^6 s^{-1}.[24] It is of interest to compare this value with that estimated from Marcus theory.[27,28]

$$k_{et} = \frac{4\pi^2}{h} H_{AB}^2 \frac{1}{(4\pi\lambda RT)^{1/2}} = \exp\frac{(-\Delta G^{0\prime} + \lambda)}{4\pi RT}$$

In this equation, H_{AB} describes the electronic coupling between the redox centers which is strongly dependent on distance, $\Delta G^{0\prime}$ is the driving force, and λ is the reorganization energy. In addition to distance, H_{AB} is dependent on the protein matrix between redox centers, which has led to a dominant pathway model where electronic coupling involves a combination of electron transfer through covalent and noncovalent bonds in addition to through space jumps,[29] which is readily known from the crystal structure. Unfortunately a number of these parameters, especially λ, must be estimated and the resulting computed rate is 3×10^5 s^{-1}, which is about 8-fold lower than experiment.[24] It is somewhat in the eye of the beholder how good the agreement is between theory and experiment, but given the uncertainty of some of

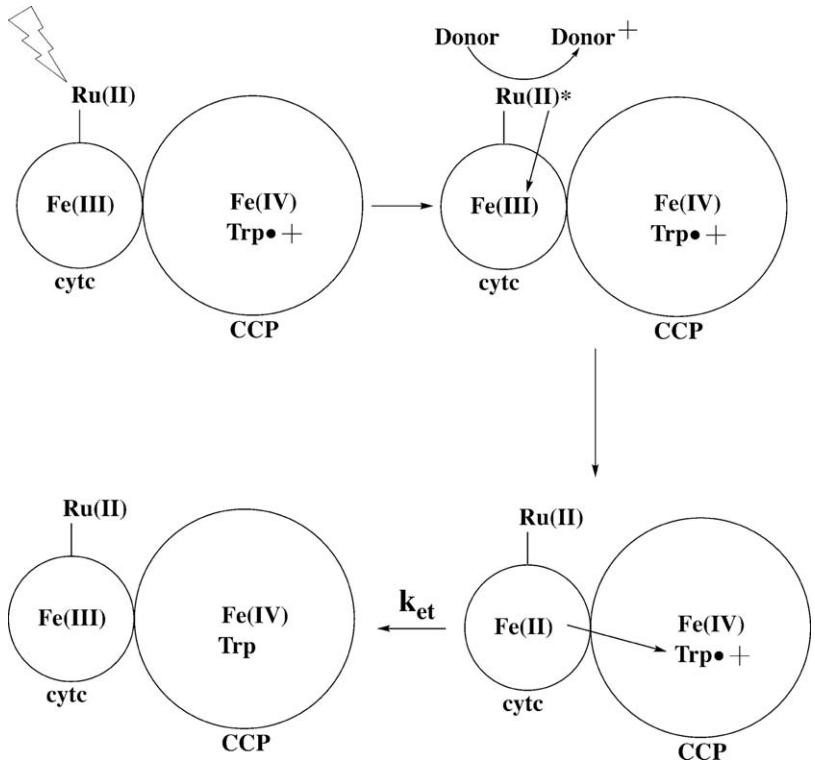

Figure 2.6 The laser excitation method used by Millet and coworkers[30] to measure the rate of electron transfer from cytc to CCP Compound I. Cytc is selectively labeled with a Ru compound that is sensitive to photo-excitation. The excited Ru(II)* transfers an electron to the cytc heme iron. A sacrificial electron donor is required to ensure that the Ru(III) produced is back-reduced to Ru(II) in order to prevent back electron transfer from the cytc Fe(II) to Ru(III). This enables the rate of interest, k_{et}, to be measured.

the estimates that must be made, a factor of 10 when the rates are so high is reasonably good. How Fe(IV)=O is reduced is less clear. The weight of the evidence favors reduction of Trp191$^{\bullet+}$ in both electron transfer steps, which requires electron transfer from Trp191 to Fe(IV)=O to regenerate the Trp191$^{\bullet+}$ radical and Fe(III) as shown in Figure 2.7.[30] Although consistent with much of the published work, the mechanism shown in Figure 2.7 does have some remaining problems. Most important is the Trp191 to Fe(IV)=O electron transfer reaction. Attempts to study this reaction give rates that are too slow to account for turnover. There are a variety of ways to work around this problem such as invoking a concerted electron transfer process from cytc to Fe(IV)=O through a transient Trp191$^{\bullet+}$ radical or a conformational sub-state that is populated only when cytc binds and favors reduction of Fe(IV)=O by Trp191. These explanations, however, are speculative although Figure 2.7 shows the current best working model.

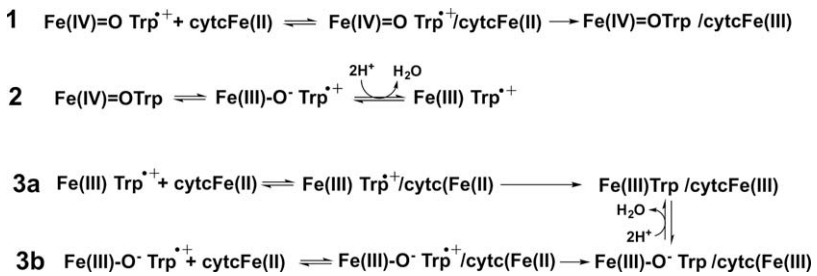

Figure 2.7 The overall catalytic cycle of CCP. It has been established that the Trp191 radical is required for both electron transfer reactions, which further requires the equilibrium in step 2. The reduction of Fe(IV) by Trp191 has been the most challenging part of the cycle to study.

These many studies on CCP, both steady state and transient state kinetics, have resulted in a comprehensive analysis of the overall mechanism,[22,31] which is summarized as follows. CCP has weak and strong binding sites for cytc. The strong site is the same one observed in the crystal structure and, as noted earlier, is also the only site competent in electron transfer. The weak site is important only at low ionic strength where cytc binding at the weak site promotes dissociation of cytc from the strong site. At low ionic strength the complex is especially strong so dissociation of cytc is rate limiting. At high ionic strength the weak site is no longer important and the rate limiting step shifts to reduction of Fe(IV)=O. Since both electron transfer steps require reduction of Trp191$^{\bullet+}$,[32] then intramolecular electron transfer from Trp191 to Fe(IV)=O is critical (Figure 2.7, step 2) and this step is limiting at high ionic strength. The main stumbling block in this mechanism is that the rate of intramolecular electron transfer between the iron and Trp191 to go from Fe(IV)=OTrp to Fe(III)Trp$^{\bullet+}$ is too slow to account for steady state rates.[32] Reduction of the Fe(IV)=O center, however, is a complex process as illustrated in Figure 2.7. Reduction of Fe(IV)=O by Trp191 results in Fe(III)-O$^-$, which is then protonated to give Fe(III) plus water (Figure 2.7, step 3a). Wang *et al.*[24] suggest that the slow step could be bypassed if the reduction of Fe(IV)=O proceeds as shown in Figure 2.7 step 3b where electron transfer occurs before protonation of Fe(III)-O$^-$.

2.5 The CCP Trp Radical

A unique feature of yeast CCP and very likely other mitochondrial CCPs (see next section) is the very stable Trp$^{\bullet+}$ radical formed in Compound I. Both computational and protein engineering approaches show that the local electrostatic environment around Trp191 stabilizes the positive charge on Trp$^{\bullet+}$ (reviewed in ref. 33). The effects of modulating the local electrostatic environment are complex and greatly influenced by ionic strength. Most importantly, various mutants that were designed to decrease electrostatic stabilization of Trp191$^{\bullet+}$ also decrease activity but only at high ionic

strength.[34] This is very likely because the rate limiting step changes with increasing ionic strength and by assuming that a full equivalent of $Trp191^{\bullet+}$ forms even in the mutants. As noted in the previous section, the rate limiting step at low ionic strength is dissociation of cytc but at high ionic strength, the rate limiting step is intramolecular electron transfer from Trp191 to Fe(IV)=O. Therefore, at high ionic strength the stability of $Trp191^{\bullet+}$ is much more important and thus, those mutants with an unstable $Trp191^{\bullet+}$ are less active at high ionic strength. Again this assumes that even in the mutants where $Trp191^{\bullet+}$ is destabilized, Trp191 is still fully oxidized but is too unstable to support high turnover at high ionic strength where $Trp191^{\bullet+}$ stability plays a much more important role in the rate limiting step.

These observations provided the basis for experiments designed to time the lifetime of the $Trp191^{\bullet+}$.[35] In these experiments, CCP is converted to Compound I by rapid mixing with H_2O_2 followed by mixing with reduced cytc and the rate and extent of cytc oxidation is measured. Between the two mixes is a delay time. The longer the delay time, the less $Trp^{\bullet+}$ radical and the less cytc is reduced. These experiments showed that mutants with a destabilized $Trp191^{\bullet+}$ oxidize less cytc at a slower rate as the delay time increased. However, if Tyr236 (Figures 2.2 and 2.8) was converted to Phe then the mutants behaved like wild type CCP at very short delay times. After a few seconds' delay time, the mutant was effectively inactive. Tyr236 is near Trp191 and is known to provide a secondary site of radical formation in Compound I.[36] Without Tyr236, the radical center is kinetically trapped on Trp191 even though its stability has been decreased in the mutants. In other words, the ''road out'' for $Trp191^{\bullet+}$ decay has been blocked and thus equilibration with other more stable sites is slow. CCP thus has proven to be

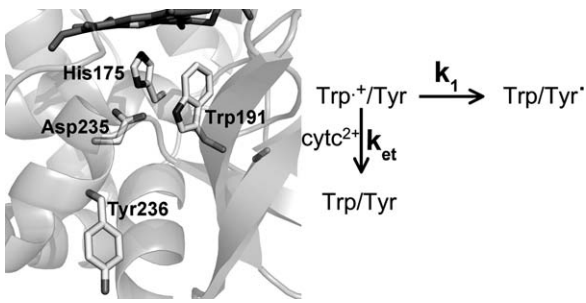

Figure 2.8 A model of radical movement in CCP Compound I based on double stopped flow experiments.[35] In mutants where the Trp191 radical is unstable, Trp191 is initially fully oxidized but the radical then migrates rapidly to other Tyr residues with Try236 providing the main path of radical migration. The level of activity depends on the relative rates of k_1 and k_{et}. When Tyr236 is changed to Phe, k_1 slows and the radical becomes kinetically trapped on Trp191 so activity is higher. With longer delay times, the radical migrates out and the extent of cytc oxidation decreases.

an unexpectedly valuable system for studying aromatic radical formation, stability, and migration in proteins.

2.6 Other CCPs

For quite some time, yeast was the only organism known to have a CCP. In the current era of genome sequencing, however, we now know that yeast is not alone. A simple BLAST search shows that various parasitic protozoa such as *Leishmania major*, *Trypanasoma cruzi*, and *Angomonas deanei* have a CCP-like enzyme. The most well characterized of these is the *L. major* peroxidase, abbreviated LmP. Initial characterization of LmP suggested that this might be an ascorbate peroxidase[37] but it was later shown to be a CCP.[38] LmP is very similar to yeast CCP in both activity and formation of a very stable Trp radical although there are some noteworthy differences. LmP, in common with many other peroxidases except yeast CCP, has a cation bound about 8 Å from the site of Trp radical formation. As noted earlier, engineering this cation into yeast CCP decreases stability of the $Trp191^{\bullet+}$ so it was unexpected to find that LmP has the cation bound but still forms a very stable $Trp208^{\bullet+}$ radical.[39] One obvious difference is that LmP has Cys197 near Trp208 (Figure 2.9) where yeast CCP has Thr180 (Figure 2.9). Mutagenesis studies showed that Cys197 plays a major role in stabilizing the Trp208 radical.[39] Another significant difference is that LmP exhibits simple Michaelis–Menten kinetics while yeast CCP is more complex. There are breaks in Eadie–Hofstee plots with CCP15 suggesting two cytc binding sites while with LmP there is no break (Figure 2.2). In addition, yeast CCP activity first increases with ionic strength and then decreases while LmP exhibits a steady decrease (Figure 2.2). This suggests that the LmP–cytc interaction relies more heavily on ionic interactions and that there is no secondary cytc binding site that effects enzyme kinetics.

2.7 LmP–cytc Crystal Structure

The LmP–cytc crystal structure[40] provides a structural basis for some of the differences observed with yeast CCP. Unlike in the yeast complex, there are direct inter-protein ion pairs formed in the LmP–cytc complex (Figure 2.4). Arg24 in cytc interacts with Asp211 in LmP while on the periphery of the complex, Lys98 in cytc interacts with Glu49 in LmP. In order for the Arg24–Asp211 ion pair to form, Arg24 must adopt a new rotamer orientation that results in the rupture of an intramolecular ion pair between Arg24 and a cytc carboxylate. The cytc Arg24Ala mutant exhibits about 2% wild type activity, which underscores the importance of this interaction.[40] The more critical role played by ionic interactions in the LmP–cytc complex compared to the more important role of nonpolar interactions in the yeast CCP–cytc complex requires a difference in how the cytc is oriented relative to the peroxidase (Figure 2.4). These differences in interaction are due primarily to variations in the peroxidases and not the cytcs so it appears that Nature can tolerate

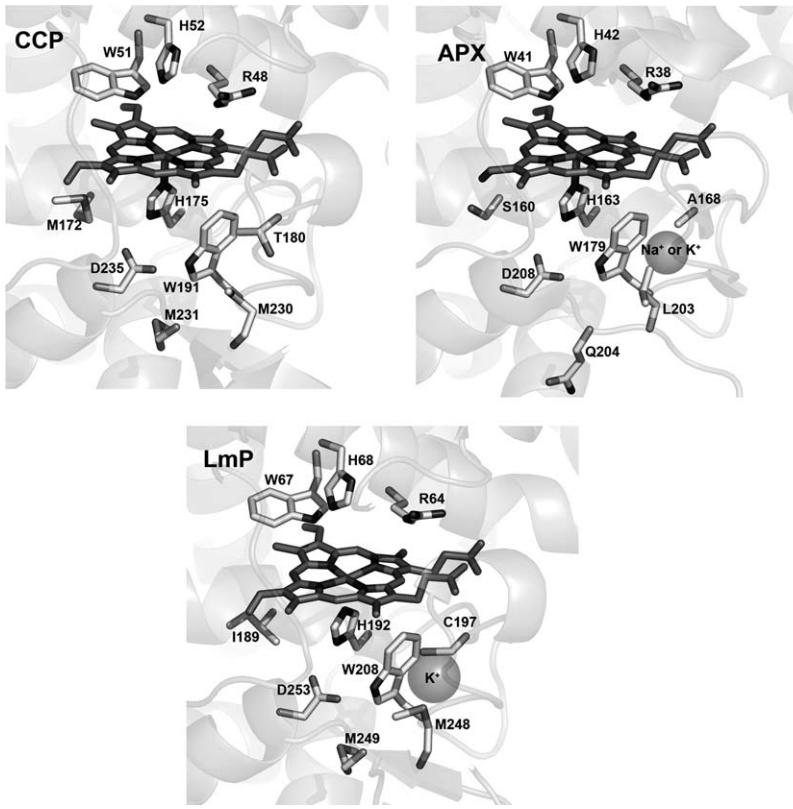

Figure 2.9 The crystal structure of the three closely related peroxidases showing the location of a cation about 8 Å from the proximal side Trp that forms a cationic radical in CCP and LmP. Of the three, CCP is the only one that lacks a cation.

changes in the peroxidase without compromising complex formation and activity. Despite the differences in contacts, the surfaces that interact are basically the same as are the contacts between the cytc heme and peroxidase protein, and electron transfer distance.

2.8 Summary and Conclusion

The CCP–cytc system is one of the most thoroughly investigated biological electron transfer systems. In part, this is due to the ease of preparing large amounts of protein for detailed biophysical analysis, the tolerance of each protein to mutagenesis, and the unusual stability of Compound I, which has enabled a detailed study of the Trp radical and ferryl center. In addition, the CCP–cytc system had an historical advantage since CCP was, for some time, the only cytc redox partner enzyme where the crystal structure was known. CCP was also one of the first heme enzymes to be recombinantly expressed,[41] which opened the way to extensive protein engineering studies.

More recently, NMR[17,42] has provided important insights into the dynamics of complex formation. The most recent advance has been the determination of the LmP–cytc crystal structure.[40] As might be expected, the complex is very similar to the CCP–cytc complex and while the orientation of cytc relative to the peroxidase is slightly different, the electron transfer path and distance between redox centers is the same. This strongly supports the view that there is only one active redox complex in the family of mitochondrial CCPs. Even so, the detailed interactions at the complex interface are quite different with electrostatics playing a more dominant role in LmP. Based on sequence alignments, the more important role nonpolar interactions play in yeast CCP may be an exception to the rule. LmP also appears to be a simpler system in that there is so far no indication of a second binding site for cytc and LmP follows simple Michaelis–Menten kinetics at all ionic strengths. This should make it somewhat easier to test various models of redox complex formation and better correlate mutagenesis studies with kinetics. Given that many of the new CCPs are from important pathogens, there could well be a higher incentive to more deeply probe the biological role of CCP. For example, the *L. major* LmP knock-out clearly shows that LmP is important in protecting the parasite from oxidative stress.[43] If LmP is a representative example of other pathogen CCPs, then the simpler kinetics and biological importance should encourage further studies on LmP-like CCPs.

References

1. A. N. Volkov, P. Nicholls and J. A. Worrall, *Biochim. Biophys. Acta*, 2011, **1807**, 1482–1503.
2. A. M. Altschul, R. Abrams and T. R. Hogness, *J. Biol. Chem.*, 1940, **136**, 777–794.
3. T. Yonetani, *Enzymes*, 1976, **13**, 345–361.
4. D. Dolphin, A. Forman, D. C. Borg, J. Fajer and R. H. Felton, *Proc. Natl. Acad. Sci. U. S. A.*, 1971, **68**, 614–618.
5. T. Yonetani, H. Schleyer and A. Eherenberg, *J. Biol. Chem.*, 1966, **241**, 3240–3243.
6. A. F. Coulson and T. Yonetani, *Biochem. Biophys. Res. Commun.*, 1972, **49**, 391–398.
7. M. Sivaraja, D. B. Goodin, M. Smith and B. M. Hoffman, *Science*, 1989, **245**, 738–740.
8. T. L. Poulos, S. T. Freer, R. A. Alden, S. L. Edwards, U. Skogland, K. Takio, B. Eriksson, N. Xuong, T. Yonetani and J. Kraut, *J. Biol. Chem.*, 1980, **255**, 575–580.
9. R. Swanson, B. L. Trus, N. Mandel, G. Mandel, O. B. Kallai and R. E. Dickerson, *J. Biol. Chem.*, 1977, **252**, 759–775.
10. M. R. Mauk, J. C. Ferrer and A. G. Mauk, *Biochemistry*, 1994, **33**, 12609–12614.
11. J. S. Zhou and B. M. Hoffman, *Science*, 1994, **265**, 1693–1696.

12. T. L. Poulos, S. Sheriff and A. J. Howard, *J. Biol. Chem.*, 1987, **262**, 13881–13884.
13. H. Pelletier and J. Kraut, *Science*, 1992, **258**, 1748–1755.
14. M. Guo, B. Bhaskar, H. Li, T. P. Barrows and T. L. Poulos, *Proc. Natl. Acad. Sci. U. S. A.*, 2004, **101**, 5940–5945.
15. C. H. Kang, D. L. Brautigan, N. Osheroff and E. Margoliash, *J. Biol. Chem.*, 1978, **253**, 6502–6510.
16. X. Wang and G. J. Pielak, *Biochemistry*, 1999, **38**, 16876–16881.
17. Q. Bashir, A. N. Volkov, G. M. Ullmann and M. Ubbink, *J. Am. Chem. Soc.*, 2010, **132**, 241–247.
18. S. H. Northrup, J. O. Boles and J. C. Reynolds, *Science*, 1988, **241**, 67–70.
19. H. S. Pappa and T. L. Poulos, *Biochemistry*, 1995, **34**, 6573–6580.
20. H. S. Pappa, S. Tajbaksh, A. J. Saunders, G. J. Pielak and T. L. Poulos, *Biochemistry*, 1996, **35**, 4837–4845.
21. S. Nakani, T. Viriyakul, R. Mitchell, L. B. Vitello and J. E. Erman, *Biochemistry*, 2006, **45**, 9887–9893.
22. M. A. Miller, *Biochemistry*, 1996, **35**, 15791–15799.
23. R. Q. Liu, S. Hahm, M. Miller, B. Durham and F. Millett, *Biochemistry*, 1995, **34**, 973–983.
24. K. Wang, H. Mei, L. Geren, M. A. Miller, A. Saunders, X. Wang, J. L. Waldner, G. J. Pielak, B. Durham and F. Millett, *Biochemistry*, 1996, **35**, 15107–15119.
25. S. Hahm, M. A. Miller, L. Geren, J. Kraut, B. Durham and F. Millett, *Biochemistry*, 1994, **33**, 1473–1480.
26. S. Hahm, L. Geren, B. Durham and F. Millett, *J. Am. Chem. Soc.*, 1993, **115**, 3372–3373.
27. R. A. Marcus, *J. Chem. Phys.*, 1956, **24**, 966–978.
28. R. A. Marcus and N. Sutin, *Biochim. Biophys. Acta*, 1985, **811**, 265–332.
29. D. N. Beratan, J. N. Onuchic, J. R. Winkler and H. B. Gray, *Science*, 1992, **258**, 1740–1741.
30. F. Millett, M. A. Miller, L. Geren and B. Durham, *J. Bioenerg. Biomembr.*, 1995, **27**, 341–351.
31. H. Mei, K. Wang, S. McKee, X. Wang, J. L. Waldner, G. J. Pielak, B. Durham and F. Millett, *Biochemistry*, 1996, **35**, 15800–15806.
32. R. Q. Liu, M. A. Miller, G. W. Han, S. Hahm, L. Geren, S. Hibdon, J. Kraut, B. Durham and F. Millett, *Biochemistry*, 1994, **33**, 8678–8685.
33. T. L. Poulos, *Chem. Rev.*, 2014, **114**, 3919–3962.
34. B. Bhaskar, C. A. Bonagura, H. Li and T. L. Poulos, *Biochemistry*, 2002, **41**, 2684–2693.
35. T. P. Barrows, B. Bhaskar and T. L. Poulos, *Biochemistry*, 2004, **43**, 8826–8834.
36. R. A. Musah and D. B. Goodin, *Biochemistry*, 1997, **36**, 11665–11674.
37. S. Adak and A. K. Datta, *Biochem. J.*, 2005, **390**, 465–474.
38. V. S. Jasion and T. L. Poulos, *Biochemistry*, 2012, **51**, 2453–2460.
39. V. S. Jasion, J. A. Polanco, Y. T. Meharenna, H. Li and T. L. Poulos, *J. Biol. Chem.*, 2011, **286**, 24608–24615.

40. V. S. Jasion, T. Doukov, S. H. Pineda, H. Li and T. L. Poulos, *Proc. Natl. Acad. Sci. U. S. A.*, 2012, **109**, 18390–18394.
41. D. B. Goodin, A. G. Mauk and M. Smith, *Proc. Natl. Acad. Sci. U. S. A.*, 1986, **83**, 1295–1299.
42. S. Vanwetswinkel, N. A. J. van Nuland and A. N. Volkov, *J. Biomol. NMR*, 2013, **57**, 21–26.
43. S. Pal, S. Dolai, R. K. Yadav and S. Adak, *PLoS One*, 2010, **5**, e11271.
44. C. H. Kang, S. Ferguson-Miller and E. Margoliash, *J. Biol. Chem.*, 1977, **252**, 919–926.